Microplate Model for the Present-Day Deformation of Tibet

Wayne Thatcher » U. S. Geological Survey, Menlo Park, CA

Site velocities from 349 Global Positioning System (GPS) stations are used to construct an 11-element quasi-rigid block model of the Tibetan Plateau and its surroundings (Figure 3). Rigid rotations of five major blocks are well determined and average translation velocities of six smaller blocks can be constrained. Where data are well distributed, the velocity field can be explained well by rigid block motion and fault slip across block boundaries. Residual misfits average 1.6 mm/yr compared to typical one standard deviation velocity uncertainties of 1.3 mm/yr. Any residual internal straining of the blocks is small and heterogeneous. However, residual substructure might well represent currently unresolved motions of smaller blocks. Although any smaller blocks must move at nearly the same rate as the larger blocks within which they lie, undetected relative motions between them could be significant, particularly where there are gaps in GPS coverage. Predicted relative motions between major blocks agree with the observed sense of slip and along-strike partitioning of motion across major faults. However, predicted slip rates across Tibet's major strike-slip faults are low, only 5-12 mm/yr, a factor of 2 to 3 times smaller than most rates estimated from fault offset features dated by radiometric methods as ~2000 to ~100,000 year old. Previous work has suggested that both GPS results and low fault slip rates are incompatible with rigid block motions of Tibet. The results reported here overcome these objections.

Reference:

Thatcher, W., (2007) Microplate model for present day deformation of Tibet, J. Geophys. Res., 112, BO1401doi:10.1029/2005JB004244.

This work was supported by NASA Solid Earth Program & the U.S. Geological Survey Earthquake Hazards Program.

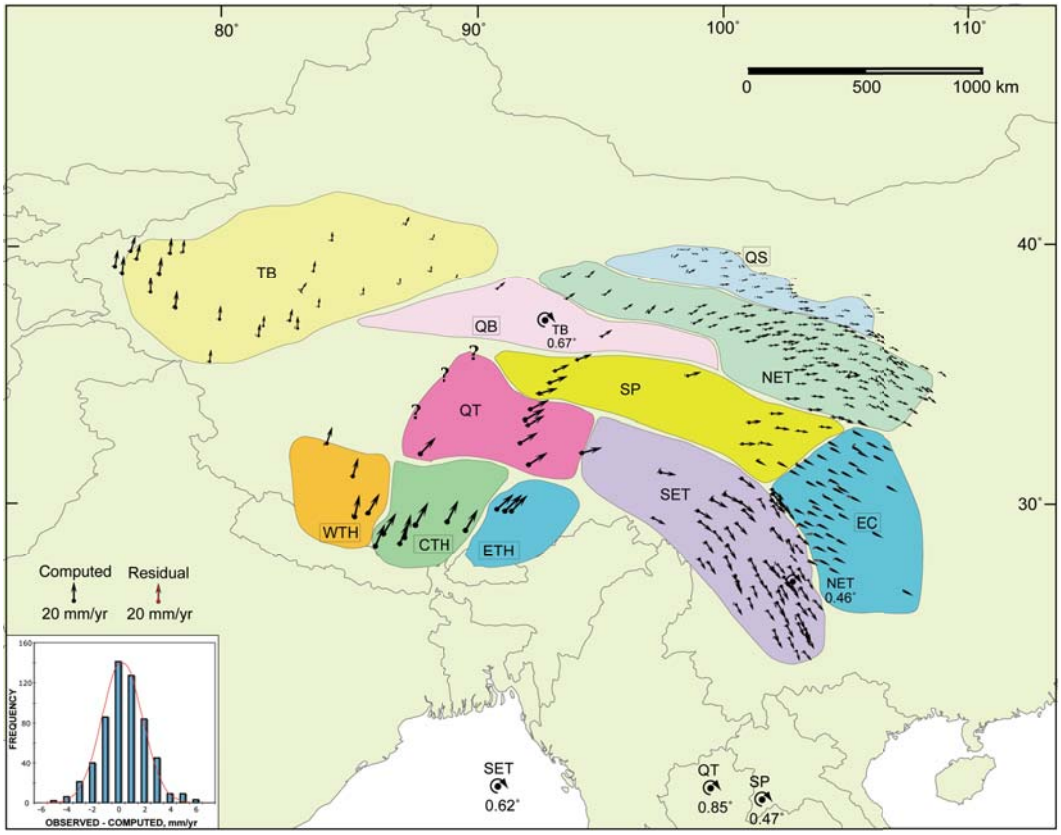

Figure 3. Predicted velocity field (black arrows) for block model of Tibet. Blocks are color-coded with abbreviated names as indicated. Smaller arrows show differences between observed and computed velocities (many are too small to be seen at true scale; these residuals are shown alone at an expanded scale in Figure 4. Inset shows histogram of residuals, which are fit well by a Gaussian distribution with mean of 0.4 and standard deviation of 1.6 mm/yr. Euler poles (rotation axes) and rotation rates (in degrees per million years) are shown for 5 blocks (NET-northeast Tibet; QT-Qiangtang; SET-southeast Tibet; SP-Songpan; TB-Tarim Basin). Average translation velocities relative to Eurasia are shown for 6 additional blocks whose abbreviated names are enclosed by rectangles (CTH-central Tibet Himalaya; EC (East China); ETH-eastern Tibet Himalaya; WTH-western Tibet Himalaya; QB-Qaidam Basin; QS-Qilian Shan). Block model parameters along with data and model fit statistics are listed in Tables 1 and 2.